Journal of Catalysis 261 (2009) 101–109

Contents lists available at ScienceDirect

Journal of Catalysis

www.elsevier.com/locate/jcat

The role of silver species on Ag/Al_2O_3 catalysts for the selective catalytic oxidation of ammonia to nitrogen

Li Zhang, Changbin Zhang, Hong He [*]

Research Center for Eco-Environmental Sciences, Chinese Academy of Sciences, P.O. Box 2871, 18 Shuangqing Road, Beijing 100085, PR China

ARTICLE INFO

Article history:
Received 23 August 2008
Revised 31 October 2008
Accepted 5 November 2008
Available online 22 November 2008

Keywords:
Selective catalytic oxidation
NH_3
Ag state
Dispersion
Particle size

ABSTRACT

The role of Ag species on Ag/Al_2O_3 catalyst for the selective catalytic oxidation (SCO) of NH_3 to N_2 was studied using 10 wt% Ag/Al_2O_3 catalysts prepared with impregnation, incipient wetness impregnation and sol–gel methods. The catalyst characterization was preformed using N_2 adsorption–desorption, UV/Vis, TEM and XRD. O_2-chemisorption and H_2–O_2 titration were measured to confirm the metal dispersion on the catalyst. The Ag species state and Ag particle size have significant influence on the Ag/Al_2O_3 activity and N_2 selectivity of the SCO of NH_3 at low temperature. Ag^0 is proposed to be an active species on the H_2 pretreated catalyst at low temperature (<140 °C). It is evident that well-dispersed and small particle Ag^0 enhances catalytic activity at low temperature, whereas large particle Ag^0 is relate to a high N_2 selectivity. In contrast, Ag^+ could also be the active species at temperatures above 140 °C.

1. Introduction

The removal of NH_3 from waste gas streams is becoming increasingly important because of environmental concerns. Selective catalytic oxidation (SCO) of NH_3 to N_2 is an ideal technology for removing NH_3 from waste gases, and it has been of increasing interest in recent years [1–3]. The application areas for the SCO of NH_3 include the treatment of waste gases from various NH_3 emission sources, such as chemical production processes, the selective catalytic reduction (SCR) of NO_x by urea for diesel powered vehicles, the purification of reformate for fuel-cell systems and the gasification/combustion of biomass for combined heat and power generation.

Previous studies showed that noble metals such as Pt, Ir and Au were active for the reaction of SCO of NH_3 at low temperature, however, the selectivity of N_2 was not satisfied for the reason that the main by-product at low temperature was N_2O [4–8]. Metal oxide catalysts, namely, MnO_2, Co_3O_4, CuO, CaO, NiO, Bi_2O_3, Fe_2O_3, V_2O_5 [9–17], and many ion-exchanged zeolite catalysts [18–22], have also been investigated for the SCO of NH_3, but NH_3 conversion levels of these catalysts at low temperature were not high enough to be of practical use.

The Ag-based catalyst used for NH_3 oxidation has been studied by some researchers previously [2,4,5,23,24]. In earlier work, Il'chenko et al. have reported that the specific catalytic activity of metal Ag at 300 °C is lower than that of the precious metals Pt and Pd [4,5]. Recently, it was reported by Gang et al. that alumina supported Ag (Ag/Al_2O_3) catalysts were extremely active for NH_3 oxidation at low temperature, and the performance of the Ag/Al_2O_3 catalyst was even superior to noble metal catalysts [2, 23]. However, the nature of Ag/Al_2O_3 for the NH_3 oxidation has not been studied in detail, such as the valence state of Ag species and particle size effect on the activity and selectivity of SCO of NH_3. In addition, the reduced Ag catalysts for NH_3 oxidation are mainly used in oxygenous environment, it is important to investigate the real performance of Ag species under reaction conditions.

In this article, we prepared the Ag/Al_2O_3 catalysts by different methods and investigated the role of Ag species on the Ag/Al_2O_3 for its catalytic activity and selectivity of NH_3 oxidation. It has been discovered that the Ag species state and Ag particle size of the Ag/Al_2O_3 have significant influence on the activity and N_2 selectivity for the SCO of NH_3. Ag^0 has been proposed as the active species at low temperature, and Ag^+ as the active species at high temperature for the SCO of NH_3, with the changeover at approximately 140 °C.

2. Experimental

2.1. Catalyst preparation and H_2 pretreatment

We prepared 10 wt% Ag/Al_2O_3 catalysts using three different methods: impregnation, incipient wetness impregnation, and sol–gel methods, denoted IM, IW and SOL, respectively. The catalysts prepared by the IM and IW methods were produced using γ-Al_2O_3 powder (250 $m^2\,g^{-1}$) with an appropriate amount of silver nitrate aqueous solution. The samples were dried at 120 °C overnight and

---

[*] Corresponding author. Fax: +86 10 62923563.
E-mail address: honghe@rcees.ac.cn (H. He).

0021-9517/$ – see front matter
doi:10.1016/j.jcat.2008.11.004

then calcined at 600 °C for 3 h in air. The preparation method for the SOL was the same as that in the literature [25] and it was calcined at 600 °C for 6 h in air. The catalysts were sieved into 20–40 mesh powders and pretreated in flowing H_2/N_2 (20 vol% H_2, 60 $cm^3\,min^{-1}$) at 400 °C for 2 h before testing.

2.2. *Catalytic tests*

2.2.1. *Catalytic activity test*

The SCO activity measurement was carried out in a fixed-bed quartz reactor. In this work, 0.2 g catalyst was used. The reactant gas was obtained by blending different gas flows. The typical reactant gas composition was as follows: 500 ppm NH_3, 10 vol% O_2, and balance N_2. The total flow rate was 200 $cm^3\,min^{-1}$ ($W/F = 0.06\ g\,s\,cm^{-3}$). NH_3, O_2, and N_2 flow rates were controlled by mass flow controllers. The inlet and outlet gas compositions were analyzed by an on-line NEXUS 670-FTIR spectrophotometer fitted with a gas cell of volume 200 cm^3. These conditions are defined as standard conditions.

In order to investigate the pre-treatment effects, we tested the activity of the fresh Ag/Al_2O_3 (IM) under the standard conditions and compared it with the activity of the H_2 pretreated Ag/Al_2O_3 (IM).

2.2.2. *Evolution with time-on-stream at 160 °C*

The H_2 pretreated Ag/Al_2O_3 (IM) catalyst was fed with the reactant mixture (standard conditions) at 160 °C, and the evolution of the NH_3 conversion and N_2 selectivity were recorded for the next 48 h at 160 °C.

2.2.3. *Temperature cycle*

The H_2 pretreated Ag/Al_2O_3 (IM) catalyst was heated from room temperature to 220 °C and cooled to room temperature under the standard conditions for 5 times.

2.3. *Characterization of catalysts*

The N_2 adsorption–desorption isotherms were obtained at −196 °C over the whole range of relative pressures, using a Quantasorb-18 automatic instrument (Quanta Chrome Instrument Co.). Specific areas were computed from these isotherms by applying the Brunauer–Emmett–Teller (BET) method. The pore size distribution was calculated by the BJH method. Before measurement, the samples were treated by degassing at 300 °C for 4 h.

Powder X-ray diffraction (XRD) measurements of the catalysts were carried out on a Rigaku D/max-RB X-Ray Diffractometer (Japan) using $CuK\alpha$ radiation and operating at 40 kV and 40 mA. The patterns were taken over the 2θ range from 20 to 70° at a scan speed of $6^\circ\,min^{-1}$.

Diffuse-reflectance UV/Vis spectra (UV/Vis) were recorded under ambient conditions on a U-3010 (Hitachi) spectrometer with a standard diffuse reflectance unit. The range was 190–850 nm and the scan rate was 300 $nm\,min^{-1}$. The measured spectra were converted into Kubelka–Munk functions and deconvoluted into Gaussian subbands that could be quantitatively assigned to the different Ag species [26–33].

Transmission electron microscopy (TEM) characterizations were carried out using an H-7500 (Hitachi) instrument. The accelerating voltage for the microscope was 80 kV and the point resolution was 0.36 nm. 200–300 particles were counted to evaluate the particle size (diameter) distribution.

The global dispersion (%) of Ag and the mean particle size (MPS) (nm) in the prepared catalysts were determined by O_2-chemisorption at 170 °C using a Quantasorb-18 (Quanta Chrome Instrument Co.) at a pressure range of 40 to 200 Torr of O_2, according to Ref. [34]. Before the O_2-chemisorption experiments, the samples were reduced in a 5 vol% H_2/Ar stream (40 $cm^3\,min^{-1}$) by heating from room temperature to 400 °C with a heating rate of 10 $°C\,min^{-1}$, and then holding at this temperature for 2 h. Metal dispersion and MPS were calculated by the Langmuir method according to a method adapted from the literature [35]. For dispersion measurements, we relied on the total adsorption isotherms and stoichiometries of $Ag/O_2 = 2$ [34,35].

H_2–O_2 titration has also been a common method for the detection of Ag dispersion. We therefore measured the Ag dispersion using a H_2–O_2 titration pulse method in a homemade pulse flow system equipped with a computer-interfaced quadruple mass spectrometer (Hiden HPR 20). Prior to the H_2–O_2 titration, 100 mg of sample was reduced in 5 vol% H_2/Ar (40 $cm^3\,min^{-1}$, 10 $°C\,min^{-1}$) at 400 °C for 2 h. Then He gas (40 $cm^3\,min^{-1}$) was passed over the sample for 1 h. After cooling to 170 °C in He, the O_2 adsorption experiment was performed, followed by flushing with He (40 $cm^3\,min^{-1}$), then the introduction of H_2 pulses (1 cm^3 of 5 vol% H_2/Ar). The stoichiometries of $Ag/O_2 = 2$, $Ag/H_2 = 1$ were assumed [34]. On the basis of these dispersion (D) data, the crystallite size could be estimated from the expression $d\ (nm) = 1.34/D$, assuming spherical Ag crystallites [36]. We note that there have been a number of studies of O_2-chemisorption and H_2–O_2 titration on Ag. We selected the reduction temperature 400 °C (10 $°C\,min^{-1}$) to ensure that the degree of reduction in these conditions was approximately 100%, the same condition as before the activity test.

3. Results

3.1. *NH_3 oxidation over 10 wt% Ag/Al_2O_3 catalysts*

To elucidate the effects of the preparation methods, 10 wt% Ag/Al_2O_3 catalysts prepared using three different methods were tested for the SCO of NH_3 at various temperatures. As can be seen in Fig. 1, IW and IM behaved similarly and they had higher NH_3 conversions at low temperature, quite different from SOL. However, the SOL showed better selectivity to N_2 than the other two catalysts. It is noteworthy that N_2O was the main by-product produced over the catalysts IM and IW at lower temperatures.

As shown in Fig. 2, H_2 pretreatment significantly improved the low temperature activity of the Ag/Al_2O_3 (IM), showing over 95% conversion of NH_3 at 140 °C and reaching 100% at 160 °C. However, no NH_3 conversion was obtained over fresh Ag/Al_2O_3 (IM) at 140 °C, but complete conversion at 220 °C.

Since the NH_3 conversion reached 100% at 160 °C over the H_2 pretreated Ag/Al_2O_3 (IM) catalyst, we kept the temperature at 160 °C for more than 48 h to continuously test the activity of the reduced Ag/Al_2O_3 catalyst (shown in Fig. 3). It was discovered that high NH_3 conversion over the H_2 pretreated Ag/Al_2O_3 at 160 °C was retained for at least 48 h, while the selectivity of N_2 increased slightly (from 46% to 50%).

As shown in Fig. 2, the NH_3 conversion over the fresh and H_2 pretreated Ag/Al_2O_3 catalysts increased with the temperature; complete conversions of NH_3 were obtained at 220 and 160 °C. Temperature cycle test was performed on the H_2 pretreated Ag/Al_2O_3 from room temperature to 220 °C for 5 times under the standard conditions. The SCO of NH_3 over the catalyst was tested at various temperatures. The result is shown in Fig. 4. It is significant that the NH_3 conversion at low temperature decreased gradually over the 5 reaction cycles, but the selectivity for N_2 formation showed the opposite behavior. In all the 5 cycles, the NH_3 conversion reached 100% at 220 °C.

We compared the performance of our Ag/Al_2O_3 catalysts with the results of the reported highly active noble metal catalysts [3,8,15] in Table 1. Since the reaction conditions of NH_3 oxidation used in these literatures were different with this work, we also

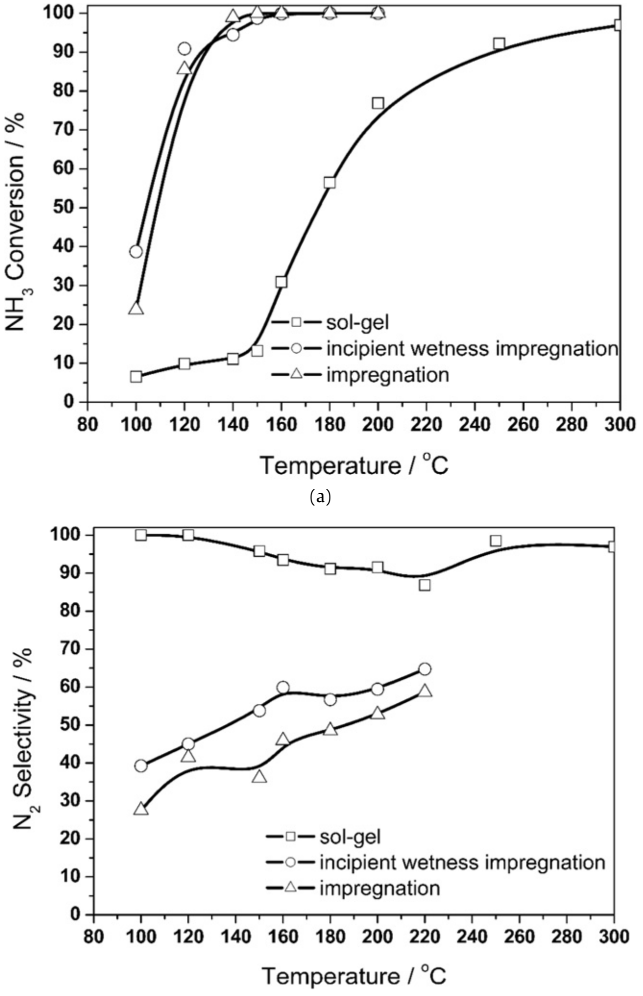

(a)

(b)

Fig. 1. NH_3 conversion (a) and N_2 selectivity (b) at different temperatures over the three H_2 pretreated 10 wt% Ag/Al_2O_3 catalysts prepared by: sol–gel (SOL), incipient wetness impregnation (IW) and impregnation (IM) methods.

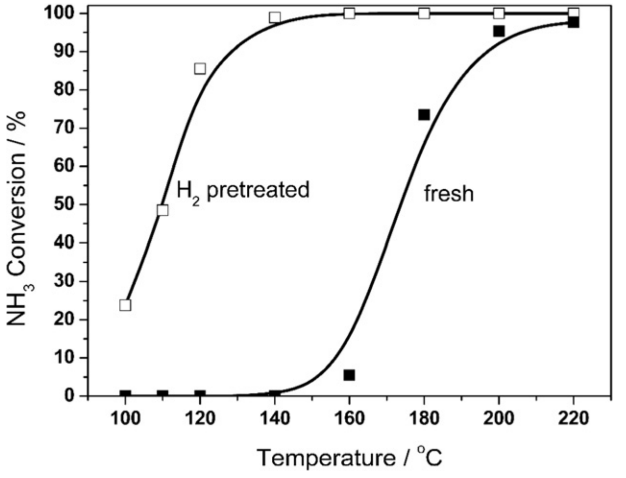

Fig. 2. NH_3 conversion over the fresh (■) and H_2 pretreated (□) 10 wt% Ag/Al_2O_3 catalysts prepared by impregnation method.

tested the activity of two noble metal catalysts prepared by impregnation method under the same conditions of this work in our laboratory. Table 1 shows the performance of the Ag/Al_2O_3 catalysts compared with the noble metal catalysts. It can be seen that the performance of Ag/Al_2O_3 catalysts (IM and IW) are superior to that of noble metal catalysts in low temperature activity as well as the Ag/Al_2O_3 (SOL) in N_2 selectivity. With further improvement, this catalyst is promising to be used instead of noble metal catalysts at low temperature (<200 °C).

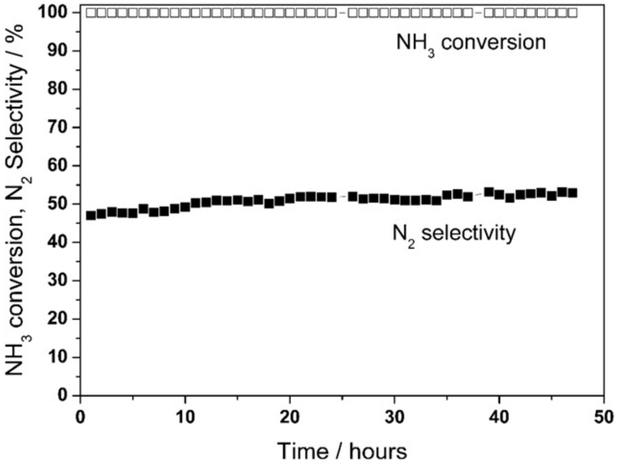

Fig. 3. NH_3 conversion (□) and N_2 selectivity (■) over the H_2 pretreated 10 wt% Ag/Al_2O_3 catalyst prepared by impregnation method (IM) at 160 °C for 48 h under the standard conditions.

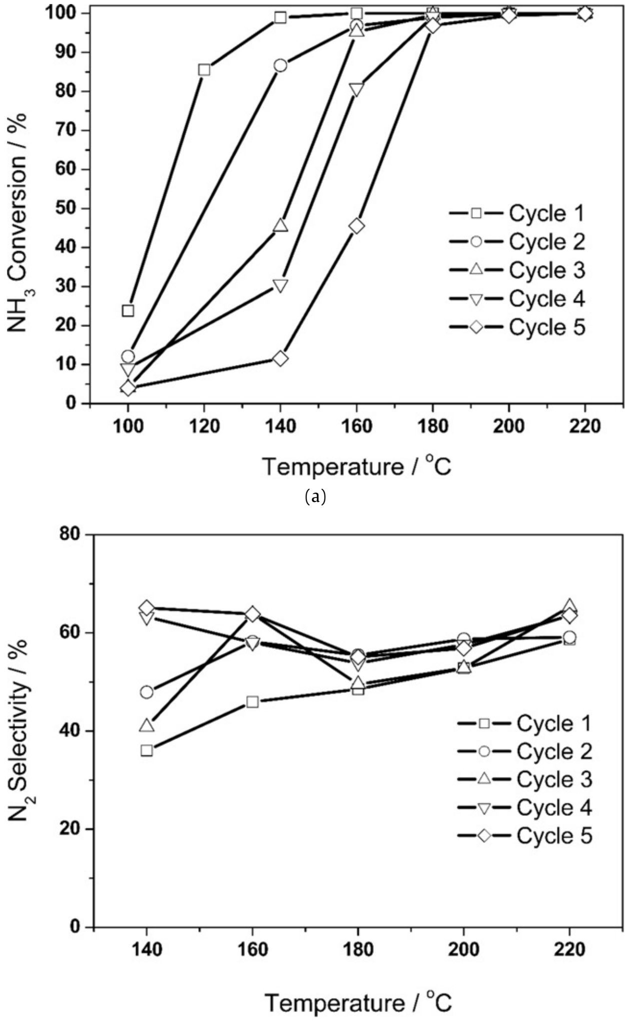

(a)

(b)

Fig. 4. NH_3 conversion (a) and N_2 selectivity (b) over the H_2 pretreated 10 wt% Ag/Al_2O_3 catalyst prepared by impregnation method (IM) over 5 cycles under the standard conditions.

Table 1
The activity and N_2 selectivity of various catalysts for NH_3 oxidation.

Catalysts	Temperature (°C)	NH_3 conversion (%)	N_2 selectivity (%)	References
10 wt% Ag/Al_2O_3 (IM)	110	48	45	This study[a]
(H_2 pretreated)	140	96	41	
10 wt% Ag/Al_2O_3 (IW)	110	52	41	This study[a]
(H_2 pretreated)	140	94	54	
10 wt% Ag/Al_2O_3 (SOL)	180	56	91	This study[a]
(H_2 pretreated)	240	90	95	
1 wt% Pd/Al_2O_3	140	34	48	This study[a]
(H_2 pretreated)[b]	160	86	75	
1 wt% Pt/Al_2O_3	220	40	76	This study[a]
(H_2 pretreated)[c]	240	83	70	
0.6 wt%	200	45	99	[3]
Pt-Fe-ZSM-5	250	99	92	
$Au/CuO/Al_2O_3$ (Cu:Al = 1:10)	211	50	94	[8]
1.2 wt% Ir/Al_2O_3	180	52	88	[15]
(H_2 pretreated)	200	100	84	

[a] Reaction conditions: NH_3, 500 ppm; O_2, 10 vol%; N_2 as balance; flow rate, 200 $cm^3\,min^{-1}$; catalyst weight, 0.2 g ($W/F = 0.06\ g\,s\,cm^{-3}$).
[b] 1 wt% Pd/Al_2O_3 prepared by impregnation method.
[c] 1 wt% Pt/Al_2O_3 prepared by impregnation method.

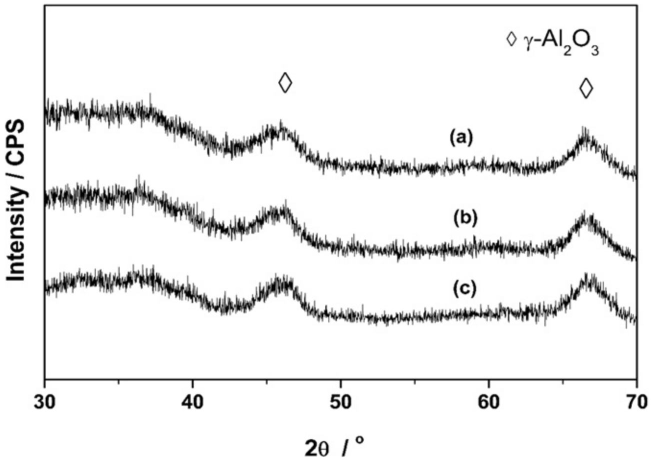

Fig. 5. XRD profiles of the fresh 10 wt% Ag/Al_2O_3 catalysts prepared by impregnation (IM) (a), incipient wetness impregnation (IW) (b) and sol–gel (SOL) (c) methods.

Table 2
BET surface area, pore size and mean particle size of the fresh 10 wt% Ag/Al_2O_3 catalysts prepared by impregnation (IM), incipient wetness impregnation (IW) and sol–gel (SOL) methods.

Catalysts	BET ($m^2\,g^{-1}$)[a]	Pore volume ($cm^3\,g^{-1}$)[a]	Average pore diameter (Å)[a]	Mean particle size (nm)[b]
IM	249	0.822	129	14
IW	248	0.709	111	14
SOL	174	0.201	42.8	21

[a] Determined by BET.
[b] Determined by TEM.

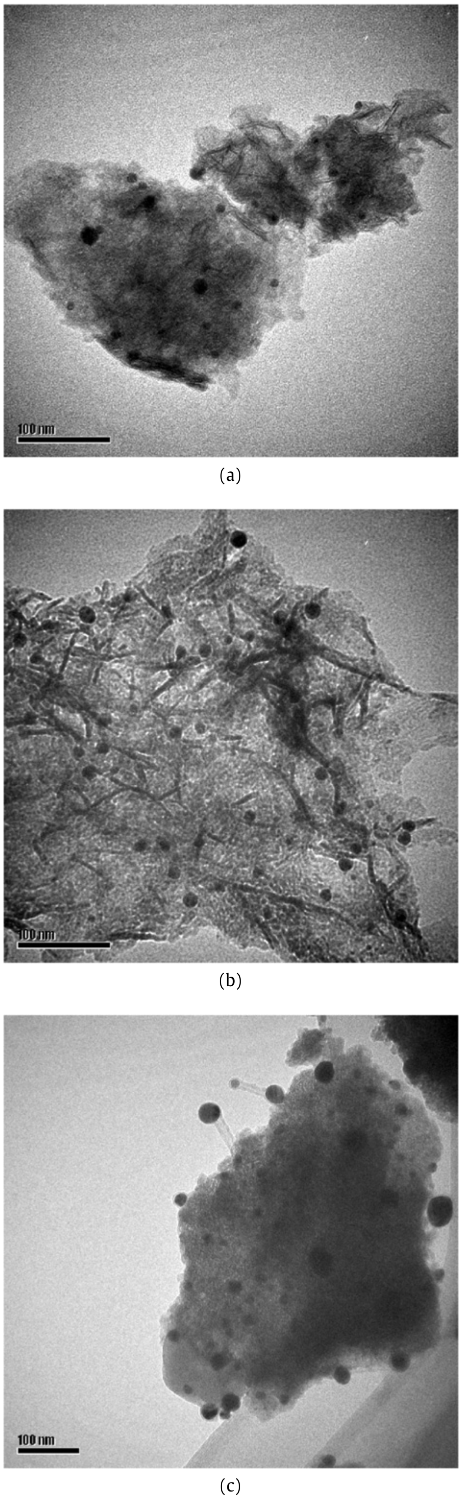

Fig. 6. TEM images of the fresh 10 wt% Ag/Al_2O_3 catalysts prepared by impregnation (IM) (a), incipient wetness impregnation (IW) (b) and sol–gel (SOL) (c) methods.

3.2. Characterization

3.2.1. X-ray diffraction

Fig. 5 shows the XRD patterns of the fresh 10 wt% Ag/Al_2O_3 catalysts prepared by the three methods. Only the γ-Al_2O_3 crystallites were evident and no Ag_2O or metallic Ag^0 crystallites appeared.

3.2.2. Transmission electron microscopy

Fig. 6 shows the TEM images of the 10 wt% Ag/Al_2O_3 catalysts prepared by the three different methods to demonstrate the distribution of Ag particles. It can be seen that small Ag particles formed on the IM and IW catalysts (Fig. 6a and b), whereas large Ag particles tended to form on the SOL catalyst (Fig. 6c). The distribution of the Ag particles on the IM and IW catalysts were similar, ranging from 3.5 to 25 nm in diameter (Fig. 6a and b), whereas there was a broad distribution on the SOL catalyst, from 12 to 50 nm in diameter (Fig. 6c). Statistical calculations on the particles measured in the TEM images were used to determine the MPS of the Ag particles on the three fresh 10 wt% Ag/Al_2O_3 catalysts (Table 2). The diameters of the particles in nanometer were calculated assuming spherical particle form. Particles under 2 nm were not detectable

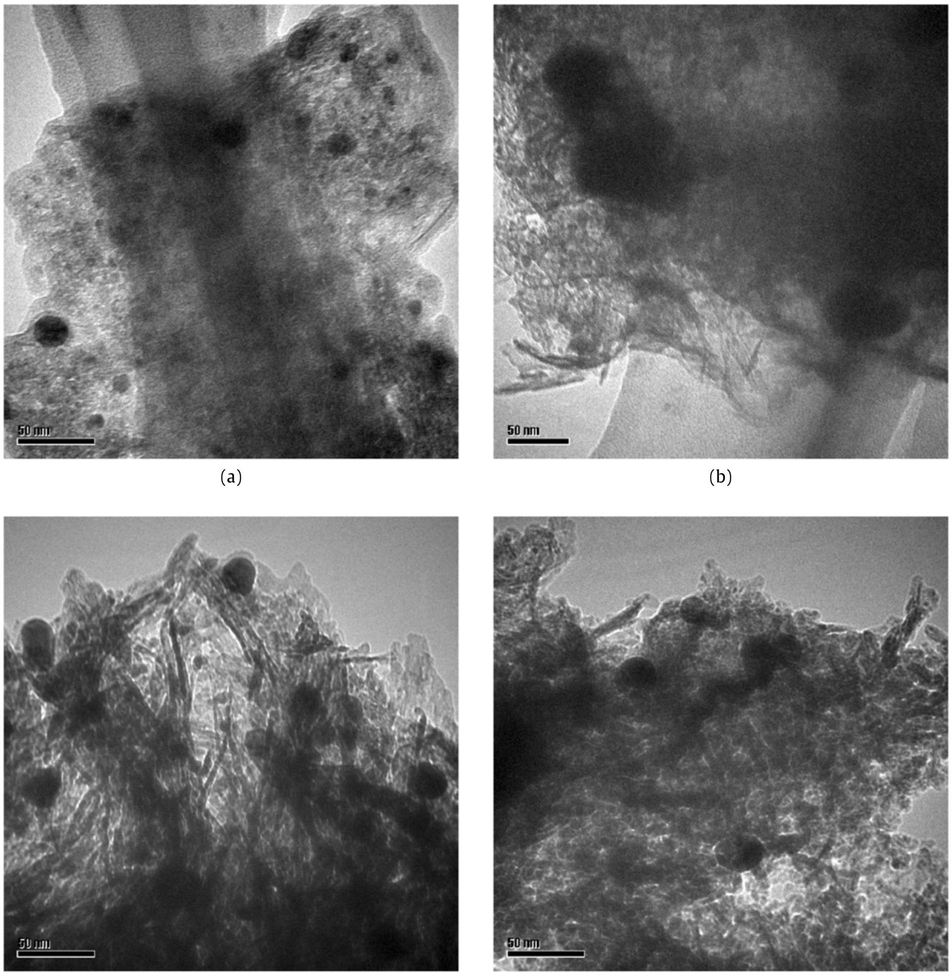

(a) (b)

(c) (d)

Fig. 7. TEM images of 10 wt% Ag/Al_2O_3 catalysts prepared by impregnation method (IM): H_2 pretreated (a); after testing at 160 °C for 48 h (b); after 1 test cycle (c); after 5 test cycles (d).

in this TEM experiment, so they have not been counted in the MPS. As shown in Table 2, the catalyst (SOL) with the lower BET surface area had a larger MPS than the other two catalysts; catalysts IM and IW with the larger surface areas had smaller MPS similarly. This demonstrates that the high surface areas of catalysts IM and IW favor the high dispersion of Ag species, thus small Ag particles are formed on the support. It also indicates that the preparation method has a significant influence on the BET surface area, pore size and Ag particle size distribution of the Ag/Al_2O_3 catalysts. Combining with our XRD spectra (Fig. 5), it clearly shows that the Ag species is well dispersed on the Ag/Al_2O_3 catalysts (IM and IW), but is not well dispersed on the SOL. However, our XRD pattern of the Ag/Al_2O_3 (SOL) (Fig. 5) shows no Ag_2O or metallic Ag^0 crystallites appeared, although the Ag particles on the SOL are quite large (12–50 nm) (Fig. 6c). This might because that Ag species on the Ag/Al_2O_3 (SOL) was amorphous phase, thus the XRD spectra could not detect it.

Fig. 7 compares the TEM images of the H_2 pretreated Ag/Al_2O_3 (IM) catalyst, a catalyst (IM) after the stability test (held at 160 °C for 48 h under standard conditions) and two cycled catalysts (IM) (tested for 1 and 5 cycles to 220 °C under standard conditions). As can be seen, some small Ag particles aggregated into larger ones after the stability test (Fig. 7b); the largest particle was about 50 nm in diameter. As shown in Fig. 7c, some Ag particles also aggregated into larger ones after 1 test cycle; the largest particle was nearly 40 nm in diameter. Aggregation of Ag particles was more evident after 5 test cycles (Fig. 7d).

The low temperature activities ($\leqslant 160\,^\circ C$) of Ag/Al_2O_3 decreased gradually over the test cycles (Fig. 4), which is coinciding with the aggregation of the Ag particles (Fig. 7c and d). It seemed that this particle size effect had an influence upon the low temperature activity. The result of the stability test showed that the 100% NH_3 conversion did not decrease after retention at 160 °C for about 50 h (Fig. 3). The TEM result (Fig. 7b) showed that some Ag particles clumped together but this did not influence the high NH_3 conversion of the Ag/Al_2O_3 at 160 °C (Fig. 3), this will be discussed in the following section. We also discovered that the Ag particle size of H_2 pretreated Ag/Al_2O_3 (IM) (Fig. 7a) was smaller than that of the fresh Ag/Al_2O_3 (IM) (Fig. 6a).

3.2.3. Diffuse-reflectance UV/Vis spectra

UV/Vis was taken to discover the details of the state of the supported Ag. Fig. 8 shows the spectra of the fresh Ag/Al_2O_3 (IM) and the three H_2 pretreated Ag/Al_2O_3 catalysts. UV/Vis analysis demonstrates the existence of different states of the Ag species, after subtraction of the Al_2O_3 spectrum. As shown in Fig. 8A, the fresh Ag/Al_2O_3 (IM) showed broad absorption bands at around 215, 275 and 350 nm, while the three H_2 pretreated Ag/Al_2O_3 catalysts gave an additional broad band at around 450 nm. The band at 215 nm is attributed to the $4d^{10}$ to $4d^95s^1$ transition of highly dispersed Ag^+ ions [28,29], 275 nm is assigned to small $Ag_n^{\delta+}$ clusters [30–32] and the bands at 350 and 450 nm are attributed to metallic silver (Ag^0) particles [28–32]. Sato et al. confirmed an absorption band of metallic Ag_n clusters at 352 nm for 4% Ag/Al_2O_3 [30]. Bog-

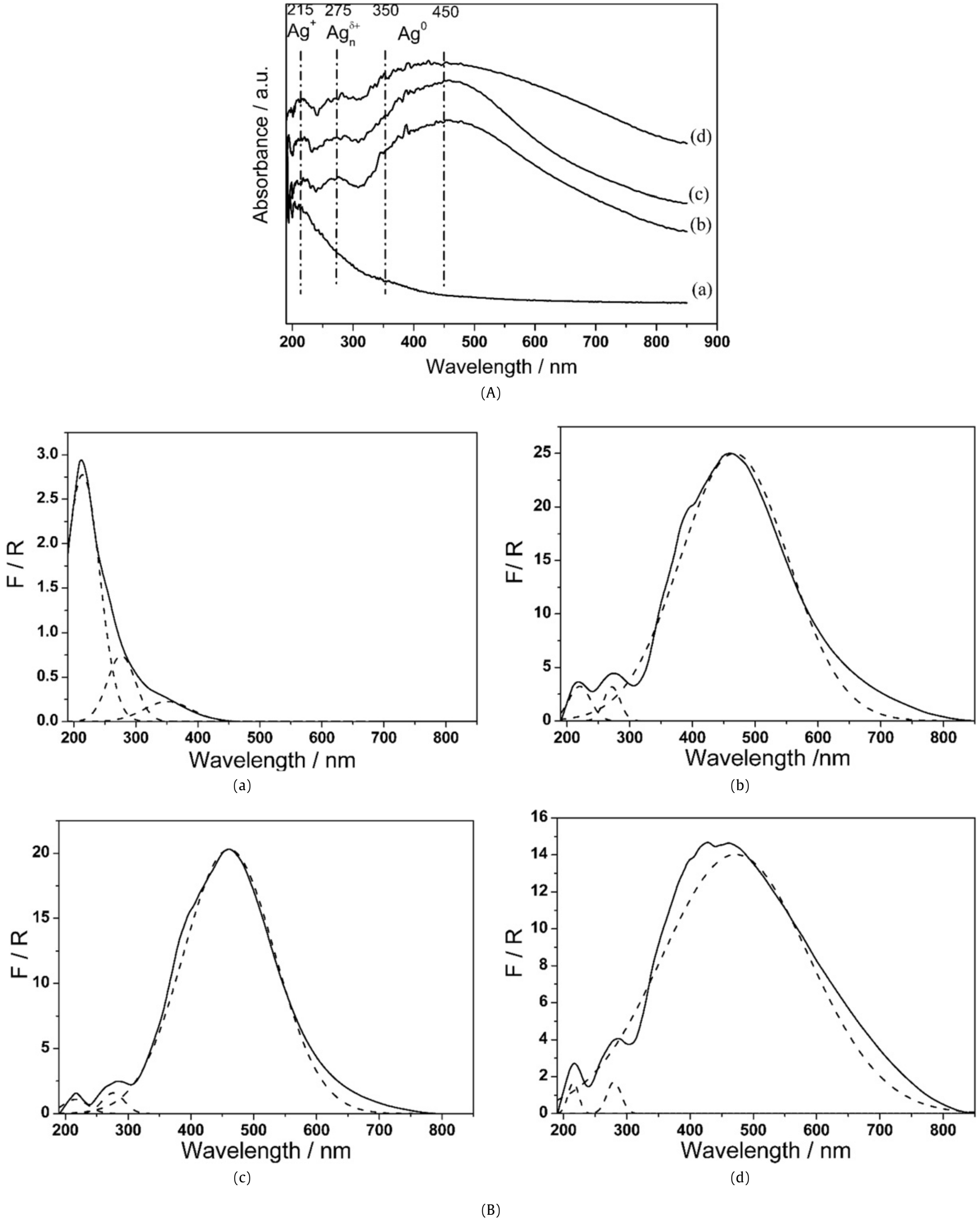

(A)

(a)

(b)

(c)

(d)

(B)

Fig. 8. Diffuse reflectance UV/Vis spectra (A) and deconvoluted subbands (B) of the fresh 10 wt% Ag/Al_2O_3 prepared by impregnation method (IM) (a) and three H_2 pretreated catalysts prepared by IM (b), incipient wetness impregnation (IW) (c) and sol–gel (SOL) (d) methods.

danchikova et al. also reported an absorption band of Ag^0 at a wavelength >390 nm for reduced Ag/Al_2O_3 [29]. Accordingly, we can estimate that the bands at 350 and 450 nm are due to metallic Ag^0 particles.

As shown in Fig. 8B, the measured spectra of the Ag/Al_2O_3 catalysts were converted into Kubelka–Munk functions and deconvoluted into Gaussian subbands that could be assigned to different Ag species [26–33]. The deconvolution was carried out based on the above assignments and the relative intensities of these subbands are listed in Table 3, including the corresponding percentage of the different Ag species. We estimated the amount of the different Ag species by multiplying the relative subband intensities by the total Ag content (10 wt%) in the Al_2O_3. The quantification of the different Ag species is shown in Table 3 as follows: I_1 for Ag^+ ($\lambda < 238$ nm), I_2 for $Ag_n^{\delta+}$ ($238 < \lambda < 320$ nm), and I_3 for Ag^0 ($\lambda > 320$ nm). However, these subbands should be understood as a description of a semi-quantitative distribution of different Ag species. Despite the uncertainty of the deconvolution procedure, the quantification in Table 3 provides a valuable indication of the relative amount of various Ag species among the catalysts investigated.

Table 3
The percentage of integrated area of the bands derived from deconvolution of the UV/Vis spectra in Fig. 8 and the corresponding Ag species dispersion on fresh and H_2 pretreated 10 wt% Ag/Al_2O_3 samples prepared by impregnation (IM), incipient wetness impregnation (IW) and sol–gel (SOL) methods.

Catalysts	Ag^+		$Ag_n^{\delta+}$		Ag^0	
	I_1[a] (%)	wt%	I_2[b] (%)	wt%	I_3[c] (%)	wt%
Fresh Ag/Al_2O_3 (IM)	71.5	7.15	19.6	1.96	8.9	0.89
H_2 pretreated (IM)	2.4	0.24	1.8	0.18	95.9	9.59
H_2 pretreated (IW)	1.3	0.13	1.8	0.18	96.9	9.69
H_2 pretreated (SOL)	0.9	0.09	1.2	0.12	98.0	9.80

[a] I_1 for Ag^+ (band at $\lambda < 238$ nm).
[b] I_2 for $Ag_n^{\delta+}$ (band at $238 < \lambda < 320$ nm).
[c] I_3 for Ag^0 (band at $\lambda > 320$ nm).

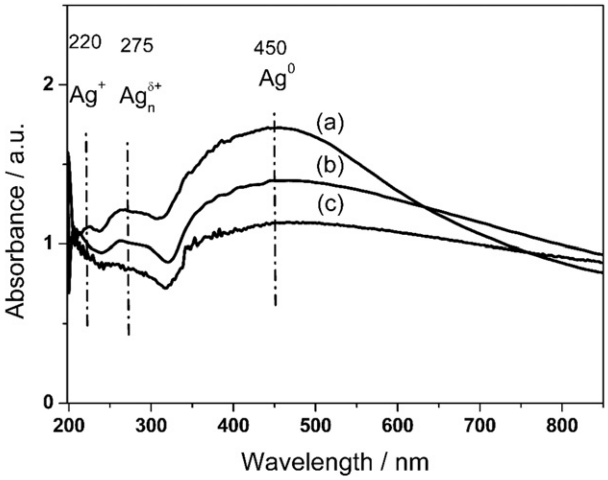

Fig. 9. Diffuse reflectance UV/Vis spectra of 10 wt% Ag/Al_2O_3 catalysts prepared by impregnation method (IM): after the stability test (held at 160 °C for 48 h) (a); after 1 test cycle (b) and after 5 test cycles (c).

For fresh Ag/Al_2O_3 (IM), Ag^+ is the major Ag species on the Al_2O_3. For the three H_2 pretreated catalysts, Ag^0 is the main Ag species on the support (Table 3). This proves that most of the Ag_xO on the Al_2O_3 can be reduced to Ag^0 by H_2 pretreatment. Combining with our activity test result (Fig. 2), the appearance of Ag^0 should be the reason for the improvement of NH_3 conversion at low temperature. Although Ag^0 is the main Ag species on the three H_2 pretreated catalysts, one can still see that the three catalysts showed different behavior for the SCO of NH_3 (Fig. 1), and this will be discussed in the following section.

Fig. 9 shows the UV/Vis result of the Ag species in the Ag/Al_2O_3 catalysts (IM) after the cyclic (room temperature −220 °C) and stability tests (160 °C). Table 4 compares the relative percentage of the Ag species of the three Ag/Al_2O_3 catalysts. It is evident that some Ag^0 species were oxidized to Ag^+ after 1 test cycle, and this is more evident after 5 cycles. Combining the cyclic test (Fig. 4) and TEM (Figs. 7c and 7d) results, we discovered that besides the Ag particle size effect, Ag^0 oxidation was another important reason for the variation of NH_3 conversion and N_2 selectivity at low temperature. However, Ag^0 was hardly oxidized after testing at 160 °C for about 50 h (Table 4). According to our stability test result (Fig. 3), the NH_3 conversion at this condition did not decrease either. These results also indicate that Ag^0 is the main active species on the H_2 pretreated Ag/Al_2O_3 (IM) at this temperature, and that the metallic Ag^0 was retained at this condition. The TEM (Fig. 7b) result showed that some Ag^0 particles aggregated together, while the high NH_3 conversion could be retained at 160 °C. This reason may be that the Ag active sites are still enough for the high NH_3 conversion in spite of the aggregation of some Ag^0 particles. In fact, we observed the decreases of NH_3 conversion with aggregation of Ag^0 particles in higher gas hourly space velocity (GHSV) experiments.

Table 4
The percentage of integrated area of the bands derived from deconvolution of the UV/Vis spectra in Fig. 9 and the corresponding Ag species dispersion on H_2 pretreated 10 wt% Ag/Al_2O_3 samples (prepared by impregnation method) after cyclic and stability tests.

Catalysts	Ag^+		$Ag_n^{\delta+}$		Ag^0	
	I_1[a] (%)	wt%	I_2[b] (%)	wt%	I_3[c] (%)	wt%
Tested 1 cycle	15.0	1.50	8.0	0.80	77.0	7.70
Tested 5 cycles	19.3	1.93	14.4	1.44	66.3	6.63
After stability test	4.8	0.48	4.0	0.40	91.2	9.12

[a] I_1 for Ag^+ (band at $\lambda < 238$ nm).
[b] I_2 for $Ag_n^{\delta+}$ (band at $238 < \lambda < 320$ nm).
[c] I_3 for Ag^0 (band at $\lambda > 320$ nm).

3.2.4. O_2-chemisorption and H_2–O_2 titration

The Ag dispersion on Al_2O_3 and the MPS of the three H_2 pretreated Ag/Al_2O_3 catalysts shown in Table 5 were determined by O_2 adsorption and H_2–O_2 titration pulse methods, which were performed at 170 °C as suggested in the literature [34,36]. The Ag dispersions of the three catalysts, as determined by the two methods, were similar. It can be seen that the MPS of catalysts IM and IW determined from O_2 adsorption and H_2–O_2 titration was consistently smaller than that of the SOL. According to our acquired turn over frequency (TOF) for NH_3 at 110 °C (Table 5), catalysts IM and IW, with similar small MPS, displayed almost the same behavior toward NH_3 oxidation. However, catalyst SOL, with larger MPS, had a much lower activity than the others. We conclude that highly dispersed Ag^0 particles favor higher activity at low temperature.

The MPS of the H_2 pretreated catalyst determined by the O_2 adsorption and H_2–O_2 titration pulse methods (Table 5) was less than that of the fresh Ag/Al_2O_3 (Table 2), which was consistent with the TEM results (Figs. 6a and 7a). UV/Vis results indicate that Ag_xO on the Al_2O_3 could be reduced to Ag^0 after H_2 reduction, so some small Ag^0 particles appeared on the support. These new Ag^0 particles must be the reason for the MPS variation for the H_2 pretreated catalyst.

4. Discussion

H_2 pretreatment significantly improved the low temperature activity of Ag/Al_2O_3 (IM) for the SCO of NH_3 (Fig. 2). The NH_3 conversion over H_2 pretreated Ag/Al_2O_3 (IM) reached over 95% at 140 °C, while no NH_3 conversion was obtained over fresh Ag/Al_2O_3 (IM) at this temperature. Ag^0 was the major Ag species on the H_2 pretreated Ag/Al_2O_3 (Fig. 8) while Ag^+ was the main Ag species on the fresh catalyst (IM) (Table 3). We infer that Ag^0 is the active species of Ag/Al_2O_3 at low temperature (<140 °C). However, the fresh Ag/Al_2O_3 was also active at temperatures above 140 °C, therefore Ag^+ could also be the active species at these higher temperatures. This proves that the active species of Ag/Al_2O_3 might be different in different temperature ranges.

Catalysts prepared by three different methods behaved differently. Ag/Al_2O_3 (SOL) had the lowest activity but the best N_2 selectivity at low temperature. Catalysts IM and IW behaved similarly and had better activities at low temperature whereas their N_2 selectivity was not good. According to N_2 adsorption–desorption, TEM, O_2-chemisorption and H_2–O_2 titration results, catalyst (SOL) with a lower BET surface area and larger Ag^0 particles did not show good activity at low temperature. Catalysts IM and IW, with highly dispersed Ag^0 particles, had higher activity for the SCO of NH_3 at low temperature. Combining these results with the UV/Vis characterization (Fig. 8) of the three H_2 pretreated Ag/Al_2O_3 catalysts, we conclude that Ag^0 was the main Ag species on the

Table 5
Ag dispersion, mean particle size and turn over frequency (TOF)[a] of three H_2 pretreated 10 wt% Ag/Al_2O_3 catalysts prepared by impregnation (IM), incipient wetness impregnation (IW) and sol–gel (SOL) methods.

Catalysts	Dispersion (%)[b]	Mean particle size (nm)[b]	TOF 10^{-3} (s^{-1})[d]	Dispersion (%)[c]	Mean particle size (nm)[c]	TOF 10^{-3} (s^{-1})[d]
IM	30.3	3.9	0.64	34.2	3.9	0.57
IW	39.7	3.0	0.53	39.2	3.4	0.53
SOL	17.3	6.8	0.19	16.6	8.1	0.20

[a] Reaction conditions: catalyst 0.2 g; NH_3 500 ppm; O_2 10%; total flow rates 200 $cm^3\,min^{-1}$; temperature 110 °C.
[b] Determined by O_2-chemisorption.
[c] Determined by H_2–O_2-titration.
[d] The TOF here was calculated by the moles of NH_3 converted per mole of Ag in the whole catalyst per second.

three catalysts. However, their activity and N_2 selectivity for the SCO of NH_3 were still different, the main differences being their Ag dispersion and Ag^0 particle size (Table 5). Highly dispersed Ag^0 particles seemed to favor the greater activity at low temperature. In contrast, larger Ag^0 particles were related to higher N_2 selectivity.

When Ag/Al_2O_3 sample was held at 160 °C for about 50 h, Ag^0 was only slightly oxidized (Fig. 9). However, some Ag^0 particles aggregated (Fig. 7b). The NH_3 conversion over the H_2 pretreated Ag/Al_2O_3 (IM) at 160 °C did not decrease over about 50 h (Fig. 3), while the selectivity to N_2 increased slightly (from 46% to 50%) during this period. These results clearly indicate that Ag^0 is the active species in these conditions and it could be retained at 160 °C. The aggregated Ag^0 particles did not influence the high NH_3 conversion at this condition, but caused the higher N_2 selectivity.

Combining the cyclic test results (Fig. 4) with the TEM (Fig. 7) and UV/Vis characterizations (Fig. 9), we discovered that after 1 test cycle to 220 °C, some Ag^0 particles were oxidized to Ag^+ species and some un-oxidized Ag^0 particles aggregated into larger ones. After 5 test cycles, the Ag^0 particles left were gradually oxidized and the un-oxidized Ag^0 particles aggregated more obviously. The NH_3 conversion at low temperature ($\leqslant$160 °C) decreased gradually and the N_2 selectivity went up significantly, which was consistent with the oxidization of Ag^0 and the aggregation of Ag^0 particles. This phenomena proves that the oxidation of Ag^0 resulted in the decrease of active species of Ag/Al_2O_3 at the low temperature ($\leqslant$160 °C), thus the activity decreased gradually at low temperature. On the other hand, the aggregation of the left Ag^0 particles on the support is another important reason for the decrease of the low temperature activity in cycle test. But the aggregated larger Ag^0 particles also caused the enhancement of the N_2 selectivity at low temperature. However, in each cycle, the NH_3 conversion could still achieve 100% at 220 °C, as the fresh Ag/Al_2O_3 (IM). This indicates the Ag^+ could be the main active species at higher temperature and thus the high NH_3 conversion could be retained over the Ag/Al_2O_3 (IM) at high temperature (>220 °C).

It was reported that the activity of NH_3 oxidation over Ag/Al_2O_3 at low temperature was related to the catalyst's ability to take part in dissociative or non-dissociative adsorption of O_2 [2]. The molecular O_2 could be adsorbed dissociatively on the H_2 pretreated Ag/Al_2O_3. In this case, catalysts IM and IW, with high surface areas and well-dispersed Ag^0 particles, favor the dissociative adsorption of O_2. Larger Ag^0 particles on Ag/Al_2O_3 (SOL) were unfavorable for the dissociative adsorption of O_2, which resulted in a lower NH_3 conversion at low temperature. The molecular O_2 could hardly be adsorbed dissociatively on the fresh Ag/Al_2O_3. In this case, NH_3 mainly reacts with molecular O_2. The dissociatively adsorbed oxygen might contribute to high activity for the SCO of NH_3 over the H_2 pretreated catalyst at low temperature (<140 °C). According to the results above, at higher temperature (>140 °C), Ag^+ could also be an active species for the activation of NH_3 prior to reacting with the molecular O_2 at higher temperature (>140 °C). The role of different O_2 species for the SCO of NH_3 and the SCO mechanism over the fresh and H_2 pretreated Ag/Al_2O_3 catalysts will be studied further in our following work.

5. Conclusions

On the basis of the above results, we conclude that the activity of 10 wt% Ag/Al_2O_3 catalysts at different temperatures mainly relate to the states of the Ag species. Ag^0 is the main active species at low temperature (<140 °C). However, Ag^+ could also be the active species at temperatures above 140 °C. The high NH_3 conversion over the H_2 pretreated Ag/Al_2O_3 catalyst could be maintained at 160 °C for about 50 h, because the metallic Ag^0 species could be retained at this condition. In contrast, the Ag^0 species could be oxidized to Ag^+ at temperatures above 160 °C.

Ag/Al_2O_3 catalysts with high surface areas and well-dispersed Ag^0 particles favor greater activity at low temperature, whereas their N_2 selectivity is not good. A catalyst with large Ag^0 particles provides high N_2 selectivity but its activity is not good at low temperature. Both Ag particle size and the states of the Ag species are important factors that influence the activity and N_2 selectivity of the SCO of NH_3.

Acknowledgments

This work was financially supported by the National Natural Science Foundation of China (20425722) and the Ministry of Science and Technology of China (2006AA060304).

References

[1] G. Olofsson, L.R. Wallenberg, A. Andersson, J. Catal. 230 (2005) 1.
[2] L. Gang, B.G. Anderson, J. van Grondelle, R.A. van Santen, Appl. Catal. B 40 (2003) 101.
[3] R.Q. Long, R.T. Yang, Catal. Lett. 78 (2002) 353.
[4] N.I. Il'chenko, G.I. Golodets, I.M. Avilova, Kinet. Catal. 16 (1975) 1264.
[5] N.I. Il'chenko, Russ. Chem. Rev. 45 (1976) 1119.
[6] J.L. Gong, R.A. Ojifinni, T.S. Kim, J.M. White, C. Buddie Mullins, J. Am. Chem. Soc. 128 (2006) 9012.
[7] D.P. Sobczyk, E.J.M. Hensen, A.M. de Jong, R.A. van Santen, Top. Catal. 23 (2003) 109.
[8] S.D. Lin, A.C. Gluhoi, B.E. Nieuwenhuys, Catal. Today 90 (2004) 3.
[9] P. Fabrizioli, T. Bürgi, A. Baiker, J. Catal. 207 (2002) 88.
[10] L. Lietti, G. Ramis, G. Busca, F. Bregani, P. Forzatti, Catal. Today 61 (2000) 187.
[11] R.Q. Long, R.T. Yang, J. Catal. 207 (2002) 158.
[12] M. Amblard, R. Burch, B.W.L. Southward, Catal. Today 59 (2000) 365.
[13] J.M.G. Amores, V.S. Escribano, G. Ramis, G. Busca, Appl. Catal. B 13 (1997) 45.
[14] R.W. Mayer, M. Hävecker, A. Knop-Gericke, R. Schlögl, Catal. Lett. 74 (2001) 115.
[15] G. Lu, B.G. Anderson, J. van Grondelle, R.A. van Santen, Catal. Today 61 (2000) 179.
[16] L. Chmielarz, P.Kuśtrowski, A. Rafalska-Łasocha, R. Dziembaj, Appl. Catal. B 58 (2005) 235.
[17] M. Trombetta, G. Ramis, G. Busca, B. Montanari, A. Vaccari, Langmuir 13 (1997) 4628.
[18] R.Q. Long, R.T. Yang, Catal. Lett. 78 (2002) 353.
[19] R.Q. Long, R.T. Yang, J. Catal. 201 (2001) 145.
[20] G. Qi, J.E. Gatt, R.T. Yang, J. Catal. 226 (2004) 120.

[21] G. Qi, R.T. Yang, Appl. Catal. A 287 (2005) 25.
[22] R.Q. Long, R.T. Yang, Chem. Commun. (2000) 1651.
[23] G. Lu, B.G. Anderson, J. Van Grondelle, R.A. Van Santen, W.J.H. Van Gennip, J.W. Niemantsverdriet, P.J. Kooyman, A. Knoester, H.H. Brongersma, J. Catal. 206 (2002) 60.
[24] M. Yang, C.Q. Wu, C.B. Zhang, H. He, Catal. Today 90 (2004) 263.
[25] Y.M. Luo, J.M. Hao, Z.Y. Hou, L.X. Fu, R.T. Li, P. Ning, X.M. Zheng, Catal. Today 93–95 (2004) 797.
[26] J. Pérez-Ramírez, M. Santhosh Kumar, A. Brückner, J. Catal. 223 (2004) 13.
[27] J. Pérez-Ramírez, J.C. Groen, A. Brückner, M.S. Kumar, U. Bentrup, M.N. Debbagh, L.A. Villaescusa, J. Catal. 232 (2005) 318.
[28] J.Q. Lu, J.J. Bravo-Suárez, M. Haruta, S.T. Oyama, Appl. Catal. A 302 (2006) 283.
[29] N. Bogdanchikova, F.C. Meunier, M. Avalos-Borja, J.P. Breen, A. Pestryakov, Appl. Catal. B 36 (2002) 287.
[30] K. Sato, T. Yoshinari, Y. Kintaichi, M. Haneda, H. Hamada, Appl. Catal. B 44 (2003) 67.
[31] A. Keshavaraja, X. She, M. Flytzani-Stephanopoulos, Appl. Catal. B 27 (2000) L1.
[32] X. She, M. Flytzani-Stephanopoulos, J. Catal. 237 (2006) 79.
[33] K. Shimizu, M. Tsuzuki, K. Kato, S. Yokota, K. Okumura, A. Satsuma, J. Phys. Chem. C 111 (2007) 950.
[34] T.E. Hoost, R.J. Kudla, K.M. Collins, M.S. Chattha, Appl. Catal. B 13 (1997) 59.
[35] K. Arve, K. Svennerberg, F. Klingstedt, K. Eränen, L.R. Wallenberg, J.-O. Bovin, L. Čapek, D.Yu. Murzin, J. Phys. Chem. B 110 (2006) 420.
[36] M.V. Badani, M. Albert Vannice, Appl. Catal. A 204 (2000) 129.